Modeling the Impact of Climate and Vegetation on Fire Regimes in Mountain Landscapes

Journal Article

Author(s):
Schumacher, Sabine; Reineking, Björn; Sibold, Jason; Bugmann, Harald

Research article

Modeling the impact of climate and vegetation on fire regimes in mountain landscapes

Sabine Schumacher[1], Björn Reineking[1], Jason Sibold[2] and Harald Bugmann[1,*]

[1]*Department of Environmental Sciences, Forest Ecology, Swiss Federal Institute of Technology Zurich, ETH-Zentrum HG G21.3, CH-8092 Zurich, Switzerland;* [2]*Department of Geography, University of Colorado, Boulder, Colorado 80209-0260, USA;* **Author for correspondence (e-mail: harald.bugmann@ethz.ch)*

Abstract

Assessing the long-term dynamics of mountain landscapes that are influenced by large-scale natural and anthropogenic disturbances and a changing climate is a complex subject. In this study, a landscape-level ecological model was modified to this end. We describe the structure and evaluation of the fire sub-model of the new landscape model LandClim, which was designed to simulate climate–fire–vegetation dynamics. We applied the model to an extended elevational gradient in the Colorado Front Range to test its ability to simulate vegetation composition and the strongly varying fire regime along the gradient. The simulated sequence of forest types along the gradient corresponded to the one observed, and the location of ecotones lay within the range of observed values. The model captured the range of observed fire rotations and reproduced realistic fire size distributions. Although the results are subject to considerable uncertainty, we conclude that LandClim can be used to explore the relative differences of fire regimes between strongly different climatic conditions.

Introduction

Forest landscape patterns result from the interactions of the physical environment, successional processes and disturbance regimes. Anticipated climate changes for the 21st century are expected to cause shifts in species composition and changes in disturbance regimes (IPCC 2001), which makes it difficult to predict the long-term development of forest landscapes. Dynamic landscape-scale models enable us to investigate these complex systems in a quantitative, structured manner.

A wide range of landscape-scale fire models exists (Gardner et al. 1999), but they do not usu-
ally consider the fire–climate–forest interactions required to predict landscape development under variable climate regimes. Fire models based on Rothermel's (1972) mechanistic approach (e.g. Albini 1976; Finney 1998) are widespread, but they require detailed fuel and weather data. Also, landscape fire models typically do not simulate vegetation dynamics in a comparably detailed manner. Spatially explicit forest gap models that integrate fire and detailed vegetation dynamics (e.g. Keane et al. 1996) are often based on highly mechanistic fire models (Rothermel 1972; Albini 1976), which makes landscape simulations (50–100 km^2) rather tedious (cf. Keane et al. 1996).

Finally, in landscape models that use stochastic approaches to examine fire–vegetation interactions, the fire regimes are typically user-defined via parameters and are not emergent properties of the models (e.g. Baker et al. 1991; He and Mladenoff 1999b). Thus, these models have limited use for predicting climate–fire interactions under a changing climate.

The landscape model LANDCLIM was built to address some of these interactions (Schumacher et al. 2004) based on the well-established LANDIS model (He and Mladenoff 1999b). LANDCLIM includes a new, simple tree succession submodel that describes forest structure and the effects of competition and climatic as well as edaphic conditions on tree population dynamics (Schumacher et al. 2004). In the first version of LANDCLIM, large-scale disturbance processes were mostly used as implemented in LANDIS. Here, we present a new version of LANDCLIM that features a fully integrated submodel for forest fire dynamics. In the context of our research, which focuses on investigating the effects of changing climatic parameters on landscape dynamics, the requirements for the new fire model were (1) to simulate fire regime as an emergent property of climate–vegetation interactions, and (2) to simulate the influence of fire on forest dynamics.

The available models demonstrate that fire behavior as a function of climate and vegetation is well understood on a scale of hours and meters, but less so on a landscape scale (Gardner et al. 1999; Keane et al. 2004). The approach presented here is based on the knowledge and experience of these fire studies and aims to encapsulate climate, fire and forest dynamics by balancing simplicity with realism. Our specific objectives were (1) to describe the fire routine of the LANDCLIM model; (2) to test whether LANDCLIM accurately simulates vegetation composition along an altitudinal gradient in an area affected by fire today; and (3) to test whether LANDCLIM can predict fire regimes over this altitudinal gradient.

Methods

Model overview

The major modifications of LANDCLIM as compared to LANDIS (He and Mladenoff 1999b)
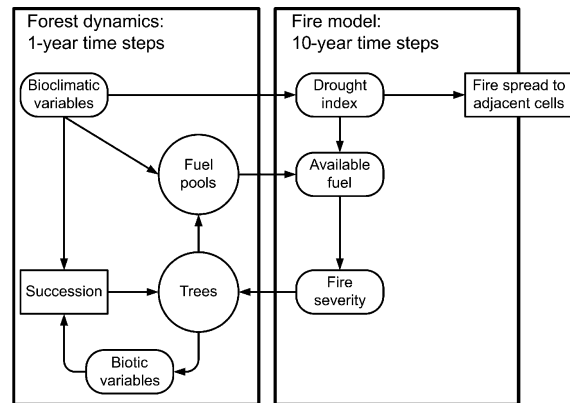

Figure 1. Overview of the structure of LANDCLIM.

include (a) quantitative descriptions of forest structure based on tree cohorts (i.e. groups of trees of the same species and age); (b) explicit incorporation of the influence of competition, climatic and edaphic parameters on tree population dynamics; and (c) modeling of the fire regime as an emergent ecosystem property based on climatic parameters and fuel load alone. LANDCLIM (cf. Figure 1) consists of a local model that simulates forest succession for each cell (usually 25 *times* 25 m) of a landscape at an annual time step, and a landscape model that simulates spatial processes operating over several cells at 10-year time steps. Landscape-scale processes in LANDCLIM are fire, windthrow, harvesting and dispersal. Since the windthrow and harvesting subroutines were not used in this study, they are not described here.

Only a brief overview of the succession model is provided here (Section 'Forest succession in LAND-CLIM') because we have previously described and tested it in detail (Schumacher et al. 2004). However, a detailed description of the fire module is given in the Section 'Fire model'.

Forest succession in LANDCLIM

Tree growth is specified as a maximum potential, which is reduced to reflect suboptimal environmental conditions (temperature, drought, light). Temperature and drought conditions (Bugmann and Solomon 2000) are determined from monthly temperature and precipitation data for each cell. Each tree species' abundance is also dependent on its ability to compete for light. Shading is simulated

based on the crown characteristics of the trees (Bugmann 1994) present per cell.

Tree mortality – In LANDCLIM, a strong reduction of growth leads to increased mortality (Schumacher et al. 2004), reflecting a stress-related decrease of tree vigor. Other factors that influence tree mortality in the model include (1) a density-dependent mortality, which occurs when stand biomass exceeds a certain level, and (2) a constant probability of death throughout tree lifespan (Botkin 1993). In addition, fire, windthrow and harvesting cause mortality.

Tree establishment – Light availability, temperature, soil moisture, browsing (Bugmann 1994) and other user-defined factors determine tree establishment potential. Establishment conditions are checked annually; however, actual establishment occurs once every decade (i.e. establishment of 10-year age cohorts, cf. Schumacher et al. 2004). Regardless of these abiotic and biotic conditions, establishment is possible only if propagules are available in the cell (cf. He and Mladenoff 1999a).

Fire model

A major assumption of the model is that fire occurrence is primarily responsive to climatic conditions (e.g. Swetnam and Betancourt 1990; Johnson 1992; Bessie and Johnson 1995). Thus, variations among fire seasons affecting fuel moisture conditions rather than fuel variables associated with stand age (e.g. amount of fuel, as implemented in the original LANDIS model) are assumed to be the most important factor determining fire occurrence. In the model, the amount of fuel has an influence on fire intensity and severity. As the flammability of fuel components depends on fuel moisture, there can be differences not only in the probability of fire occurrence but also in fire intensities between marginal and extreme fire weather years (Bessie and Johnson 1995).

Fire ignition and spread

To ignite a fire, the ignition source has to coincide with flammable fuels (Nash and Johnson 1996). In the model, a number of fire ignitions within each decade are assumed to occur at randomly selected locations to mimic lightning-caused ignitions.

Their number is controlled by a user-defined parameter; the ignition routine of LANDIS (He and Mladenoff 1999b) was used in our fire model. However, LANDCLIM determines whether an ignition source can ignite a fire at a given location in a different manner compared to LANDIS: A fire is simulated only if it can spread to a neighboring cell (i.e. the four adjacent and four diagonal cells). Whether a neighboring cell will burn depends on a fire spread probability, which represents the cell's susceptibility to fire. Thus, a fire can spread in the model until it stops expanding in all directions or reaches the boundaries of the landscape (the original LANDIS model has maximum fire size prescribed by the user).

The basic fire spread probability (*fireP*$_{base}$) is expressed as a simple function of an annual drought index (*drI*$_{an}$), which mimics average fuel dryness for any given cell [Figure 2, Eq. (1)]:

$$fireP_{base} = drI_{an}^{fireExp} \tag{1}$$

where *fireExp* is a slope parameter (Table 1). Drought conditions are determined using monthly temperature and precipitation data that are adjusted for elevation using lapse rates. The drought index is sensitive to temperature, precipitation, soil type and the topographic position of each cell, and is calculated for each fire ignition event from the annual sums of potential and actual evapotranspiration (Bugmann and
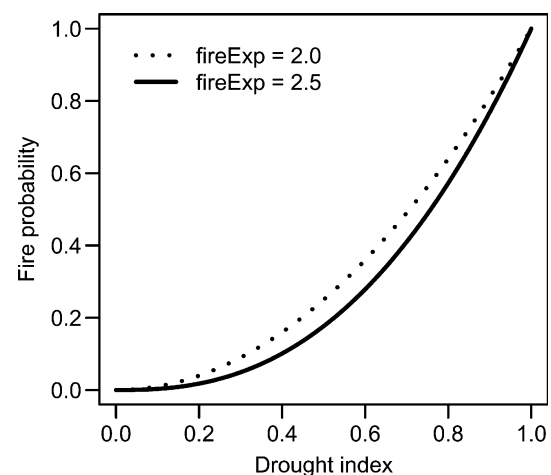

Figure 2. Fire probability (*fireP*$_{base}$) of a given cell as a function of the drought index (*drI*$_{an}$).

Table 1. Setup of simulation scenarios.

Scenario	Site	Vegetation zone	Elevation (m a.s.l.)	Area (km²)	*fireExp*
LHC2.5					2.5
	Left Hand Creek	Montane forests	1700–2700	41.2	
LHC2.0					2.0
WB2.5					2.5
	Wild basin	Subalpine forests	2600-treeline	81.7	
WB2.0					2.0

fireExp: Coefficient, fire probability [cf. Eq. (1)].

Cramer 1998) using the climate data of a randomly selected year from the past simulation decade (Schumacher 2004). Thus, climatic conditions vary between the fires simulated for the same decade.

Although the fire spread probability is independent of fuel amounts, woody fuel has to be present in a cell to support fire spread, thus preventing spread to non-forested cells.

Topography also influences fire spread: fires typically spread more easily upslope than downslope because of the pre-heating of upslope fuels (Rothermel 1972). This is taken into account by linearly increasing the spread probability by a slope adjustment factor (*sa*); downslope fire probability is reduced accordingly. However, because burning logs and other debris can roll down steep slopes and thus ignite fire downslope, the fire spread probability is reduced only up to a slope angle of 30° (Heinimann et al. 1998).

$$fireP = \begin{cases} fireP_{\mathrm{base}} \cdot (1 + sa \cdot slope) & slope > -30(^\circ) \\ fireP_{\mathrm{base}} \cdot (1 + sa \cdot -30) & \text{else} \end{cases}$$
$$(2)$$

Note that this slope adjustment [Eq. (2)] is not used to determine the initial ignition probability of a cell, where the base probability, $fireP_{\mathrm{base}}$, is used.

Wind can have a strong influence on fire behavior. These effects are not considered in the model because fire is simulated with a 10-year time step, whereas wind is characterized by dynamics operating on much smaller temporal scales. A wind adjustment coefficient could be included in Eq. (2) to distinguish windy from less windy regions; in the absence of reliable data on wind characteristics, this is however unlikely to improve model performance.

Thus, the number and size of fires simulated within each decade depends mainly on climate and topography, and varies stochastically with inter-annual climate variability.

Fuel pools

In LANDCLIM, the amount of flammable fuel determines fire impacts in burned cells. Three fuel pools are used to track the development of dead biomass: (1) Foliage (*ffl*; leaf and needle litter); (2) twigs (*twfl*; fine woody debris <7.5 cm diameter); and (3) boles (*bwfl*; wood >7.5 cm diameter). These pools change during the simulations as a result of fuel input from annual litterfall and dead trees, fuel decomposition, and fuel consumption by fire.

In the model, dead biomass results from dead trees, slash and annual litterfall. To allocate this biomass to the fuel pools, tree biomass is partitioned into foliage, twig and bole weight. Foliage weight is derived using an allometric relationship (Bugmann 1994) and is subtracted from tree biomass. Then, twig weight is estimated based on tree size, assuming that the ratio of twigs to total woody biomass decreases linearly with increasing tree size, from trees of 7.5 cm diameter at breast height (dbh) up to trees with 30 cm dbh. For trees ≥30 cm dbh, a constant fraction (*twf*, Table 2) of woody biomass is assumed to be twigs (Paulsen 1995). Bole weight is derived by subtracting twig weight from total wood weight.

All dead trees and the slash of harvested trees are partitioned as described above and added to the corresponding fuel pools. Constant fractions of total biomass are used to determine the amount of foliage, twig and bole wood slash (*fs, ts, bs*; Table 2). In addition, annual litterfall from living biomass is added to the fuel pools, calculated based on foliage retention time (*frt*) and twig turnover rate (*twtr*; Table 2).

Table 2. Default parameters used in the fire subroutine (see also Table 1).

Name	Parameter description	Value	Source
ign	Ignition coefficient	0.0002	Estimated
Sa	Coefficient, slope adjustment	0.001	Estimated
twf	Twig wood fraction (portion of twig weight of total woody biomass)	0.1	Paulsen (1995)
fs	Foliage slash fraction	1.0	Estimated
ts	Twig wood slash fraction	1.0	Estimated
bs	Bole wood slash fraction	0.05	Estimated
frt	Foliage retention time (year) Evergreen	5	Bugmann (1994)
	Deciduous	1	
twtr	Twig wood turnover rate (year^{-1})	0.03	Christensen (1977)
Lign	Average lignin content of foliage (%)	20	Meentemeyer (1978)
dec_1	Coefficient, bole wood decomp. rate	0.0166	Mackensen et al. (2003)
dec_2	Coefficient, bole wood decomp. rate	0.093	Mackensen et al. (2003)
CKbig	Crown kill threshold big trees (t/ha)	30	Estimated based on Arno (2000) and Johnson (1992)
CK small	Crown kill threshold small trees (t/ha)	5	Estimated
dbhBig	Diameter at breast height of canopy trees (cm)	40	Estimated
ck_1	Coefficient, crown kill	0.21111	See text
ck_2	Coefficient, crown kill	−0.00445	See text
tfc_1	Coefficient, twig fuel consumption	0.8	Fahnestock and Agee (1983)
tfc_2	Coefficient, twig fuel consumption	0.2	Fahnestock and Agee (1983)
bfc	Coefficient, bole fuel consumption	0.4	Fahnestock and Agee (1983)
fcr	Live foliage consumption rate	0.5	Fahnestock and Agee (1983)
tcr	Live twig consumption rate	0.1	Fahnestock and Agee (1983)
bcr	Live bole consumption rate	0.05	Fahnestock and Agee (1983)
est_{red}	Fire establishment reduction of non-adapted species (%)	90	Estimated

Biomass in the fuel pools decays according to a climate-dependent rate. The foliage litter decomposition rate (*fdr*) is based on the relationship by Meentemeyer (1978) using annual evapotranspiration, AET (mm, provided by the soil moisture routine) and leaf lignin content (*lign*, Table 2) as predictor variables:

$$fdr = \frac{-1.31369 + 0.05350 \cdot \text{AET} + 0.18472 \cdot (\text{AET}/lign)}{100}$$

(3)

A variety of decay rates for woody debris can be found in the literature (e.g. Harmon et al. 1986). In LANDCLIM, the temperature-dependent relationship by Mackensen et al. (2003) was used to calculate the decay rate of bole wood (*bdr*); twig wood was assumed to decay five times faster (*tdr*):

$$bdr = dec_1 \cdot e^{dec_2 \cdot T}$$

(4)

$$tdr = 5 \cdot bdr$$

(5)

Thus, decomposition rates vary with climate throughout a model run. Although there is usually a lag between tree death and the onset of decay, decomposition starts in the model the year after a tree dies. This simplification is justifiable, as the fire submodel operates on 10-year time steps and the onset of decay is usually much earlier than 10 years (Harmon et al. 1986). Once fuel is added to a fuel pool, it remains there until decomposed or burned. Decomposed biomass is not further accounted for in the model.

Fire effects: tree mortality

Fire leads primarily to damage of crowns and stem cambial tissue, preferentially killing trees of short stature or with thin bark. Ryan and Reinhardt (1988) found that a logistic regression based on bark thickness and the percentage of crown kill is capable of predicting the probability of fire-caused mortality across many species:

$$mP_{ire} = \frac{1}{1 + \exp(-1.466 + 1.91 \cdot BT - 0.1775 \cdot BT^2 - 0.000541 \cdot CK^2)}$$

(6)

Table 3. Species life history parameters: (a) used in the fire sub-model; (b) used in the growth sub-model (the use and relevance of these parameters is explained in Section Methods).

Name[a]	Parameter description	ABLA	PIEN	PICO	PIPO	PSME
(a)						
$bark_s$	Coefficient, bark allometry (–)	0.015	0.022	0.014	0.070	0.065
ser_s	Seeds fire adapted (–)	0	0	1	0	0
(b)						
r_s	Growth rate (year-1)	0.05	0.07	0.1	0.13	0.08
K_s	Maximum biomass (*t*)	3.3	9.7	11.3	14.0	11.2
$maxAge_s$	Maximum age (year)	300	600	600	700	700
$matu_s$	Maturity age (year)	20	40	10	10	20
ED_s	Effective seeding distance (m)	30	30	60	40	100
MD_s	Maximum seeding distance (m)	60	180	100	150	250
$folType_s$	Foliage type (–)	3	3	2	3	3
$shdTol_s$	Shade tolerance (–)	5	4	1	2	3
$minDD_s$	Minimum degree-day requirement (d)	300	400	524	1200	800
$minT_s$	Minimum temperature (°C)	−99	−99	−15	−12	−15
$drTol_s$	Drought tolerance (–)	4	4	4	6	5
$brTol_s$	Browsing tolerance (–)	1	1	1	1	1

ABLA: *Abies lasiocarpa*, PIEN: *Picea engelmannii*, PICO: *Pinus contorta*, PIPO: *Pinus ponderosa*, and PSME: *Pseudotsuga menziesii*.
[a]Sources for parameter values: *bark* (Keane et al. 1996); *ser, K, maxAge, matu, shdTol, ED, MD* (Burns and Honkala 1990; Uchytil 1991a, b; Steinberg 2002; Anderson 2003; Howard 2003); *r* (Bugmann 2001), *folType, shdTol, minDD, minT, drTol, brTol* (Bugmann 2001).

where mP_{fire} is the mortality probability of a single tree, BT is bark thickness (cm) and CK is the percentage of crown kill. Bark thickness is estimated from tree diameter using an allometric relationship ($bark_s$, Table 3), and tree diameter is derived from biomass (Schroeder et al. 1997).

The percentage of crown volume killed depends on scorch height, tree size and crown form. Scorch height is correlated with fire intensity (van Wagner 1973), which in turn is related to the amount of fuel available for combustion (Brown 2000). Crown kill (CK) is thus modeled as a function of tree size (dbh_{eff}) and available fuel ($avFuel$) [Eq. (7), Figure 3]:

$$CK = \min\left(100, 100 \cdot \left(ck_1 + ck_2 \cdot dbh_{eff}\right) \cdot avFuel\right) \tag{7}$$

where dbh_{eff} is effective tree diameter at breast height. If tree diameter is larger than $dbhBig = 40$ cm, dbh_{eff} is set to $dbhBig$ (cf. Figure 3), as we assumed that $dbhBig$ is the minimum dbh of trees that have reached the upper canopy; trees in this layer typically have comparable tree heights and crown shapes, and therefore they show the same response to fire. The values for the parameters of ck_1 and ck_2, (Table 2) were derived using the following assumptions: a threshold level of
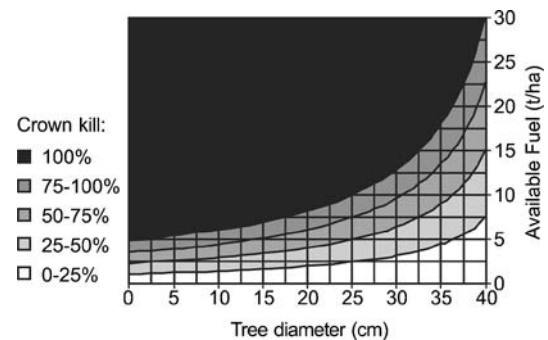

Figure 3. Percentage crown damage (*CK*) as a function of tree diameter and the amount of available fuel (*avFuel*).

available fuel (*CKbig*) is required to sustain a stand-replacing fire, i.e. a fire that is able to fully consume the crowns of large trees (*dbh > dbhBig*). Another threshold value (*CKsmall*) was defined for the amount of fuel required to cause full crown damage to the smallest trees.

Available fuel (*avFuel*) is the proportion of dead biomass that burns under given moisture conditions. The main factors affecting fuel consumption are fuel size and moisture content (e.g. Brown et al. 1991). In LANDCLIM, foliage litter consumption is assumed to be 100%, independent of its moisture content. The amount of

available woody fuel is a linear function of pre-fire loading and moisture conditions (drI_{an}, see above):

$$avFuel = ffl + (tfc_1 + tfc_2 \cdot drI_{an}) \cdot twfl$$
$$+ (bfc \cdot drI_{an}) \cdot bwfl \qquad (8)$$

where *ffl* is foliage fuel, *twfl* is twigwood fuel, *bwfl* is bolewood fuel, and *tfc$_1$*, *tfc$_2$* and *bfc* are parameters (Table 2).

Fire effects: fuel pools

Fire affects the fuel pools in two ways: (1) by reducing fuel amounts through consumption of available fuel (*avFuel*, see above); (2) by increasing fuel amounts by killed trees. Killed trees are usually only partially consumed by fire. Thus, their biomass is reduced by a consumption rate for each size class – foliage (*fcr*), twig (*tcr*), and bole (*bcr*) wood (cf. Table 2) – and the remaining biomass is added to the fuel pools.

Fire effects: tree regeneration

Fire consumes seeds on a site, but some species have specific fire adaptations (e.g. serotinous cones, buried seeds), or they can re-sprout from stumps. Species without fire adaptations are at a disadvantage, particularly if fires are frequent or large and seed sources are rare.

To include fire adaptation strategies in LANDCLIM, the number of trees potentially able to establish in a cell per decade is reduced by 90% if a fire occurred, compared to the situation without fire disturbance ($est_{red} = 90\%$). This number is not reduced for species with fire-adapted seeds ($ser_s = 1$; Table 3).

Model evaluation

To test the ability of LANDCLIM to simulate forest dynamics in the absence of fires, its performance was compared to measured data on several spatial scales in Europe (Schumacher et al. 2004). Simulations of the forest landscape in a valley in the Swiss Alps under the historic forest management regime were compared to forest inventory data (Hefti et al. 1986); simulations under natural, unmanaged conditions to data on potential natural vegetation composition (Zumbühl and Burnand 1986; Ellenberg 1996)

and the elevation of natural treeline (Körner 1998). Simulated stand–scale behavior after windthrow was compared to empirical studies (cf. Oliver and Larson 1996), data from primeval forests (Hillgarter 1971), and self-thinning studies (Yoda et al. 1963). The fire submodel described here was tested using an extensive sensitivity study (Schumacher 2004, p. 35ff.) to determine the importance of several parameters that were difficult to estimate based on literature data. As a result, the plausibility range of some parameters was determined (cf. Section 'Fire parameters' below).

Model parameterization and simulation sets

Study area and site parameters

Our study focused on two areas northwest of Boulder (CO), Colorado Front Range, USA (40.1° N; 105.5° W). Simulations were conducted in a ca. 40 km^2 area of Lefthand Creek (LHC) extending from 1720 to 2720 m a.s.l., and a ca. 80 km^2 area of Wild Basin (WB) at 2560 to 4340 m a.s.l. (Table 1).

Climate data (monthly temperature averages and precipitation sums) were from four weather stations ranging from near lower treeline to beyond upper treeline, i.e. the US Historical Climate Network site Longmont (approx. 20 km northeast of Boulder) and the Niwot Ridge LTER sites (Bugmann 2001). Altitudinal lapse rates were derived by monthly linear interpolation between the base station (Longmont) and climate stations at higher altitudes.

Soil water holding capacity was set to 10 cm across both landscapes, and the size of grid cells was 25×25 m. Elevation, slope and aspect per grid cell were derived from a digital elevation model with a resolution of 30 m (USGS).

Species-specific parameters

Five major tree species of the Colorado Front Range were parameterized in the model (*Abies lasiocarpa*, *Picea engelmannii*, *Pinus contorta*, *Pinus ponderosa*, *Pseudotsuga menziesii*) based on published data (Table 3, Bugmann 2001).

Fire parameters

Fire parameters (Table 2) were taken from published sources. Yet, some parameters could not be

derived directly from existing data, so further assumptions were made.

We were not able to quantify the relationship between site dryness and fire spread probability. Therefore, a simple function was chosen [Eq. (1)]. The shape parameter of this function, *fireExp*, was determined such that the curve would meet the percolation threshold (Stauffer and Aharony 1995) at a drought index that could be expected to support fast spreading fires over a large landscape. The corresponding drought index was initially determined based on the drought index for an extreme fire year, 2003, in Valais (Switzerland). The climate station Visp (ASTA; SMA 2003) was used, and soil bucket size was estimated as 10 cm. The resulting drought index (for 2003) was 0.67. As this was only a rough estimate, we determined the plausibility range of the shape parameter *fireExp* using a sensitivity study (Schumacher 2004). Based on these investigations and to take the inherent uncertainty into account, all simulations in this paper were performed by varying the coefficient *fireExp* to represent (a) a 'conservative' estimate of fire occurrence (*fireExp* = 2.5; simulations LHC2.5 and WB2.5); and (b) an 'extreme' estimate, i.e. the upper limit of the plausibility range (*fireExp* = 2.0; simulations LHC2.0 and WB2.0; Table 1).

Simulations

LANDCLIM was applied in the two study areas (Table 1) using full GIS information as input, but without taking current land cover type into account. Disturbances other than fire (i.e. forest management and windthrow) were excluded from the simulations.

All simulations were started from an empty landscape, with no trees in any of the cells. At the beginning of the simulations, all species were allocated a probability of 10% of contributing seeds to any cell. The model evaluation was begun after an equilibrium between climatic conditions, the disturbance regime, and vegetation structure was reached. To account for random effects, the evaluation was based on average results over the next 25,000 years (except for the WB2.5 simulation, where the fire regime was averaged over 50,000 years due to very low fire frequencies).

Results

Vegetation properties along the elevational gradient

Simulations at low altitudes in the Colorado Front Range resulted in a biomass distribution that increased from 20–120 t/ha at the lowest elevations to 250 t/ha in both LHC simulation sets (Figure 4a, b). The increase was fairly gradual in the LHC2.5 simulation (Figure 4a), whereas in the LHC2.0 simulation biomass increased only slightly over the first several 100 m (Figure 4b). Both LHC simulations resulted in a landscape dominated by *Pinus ponderosa* below 2500 m (Figure 4a, b). *Pseudotsuga menziesii* was co-dominant with increasing altitude, and *Pinus contorta* co-dominated above 2600 m in the LHC2.5 and above 2500 m in the LHC2.0 simulation.

Simulations at higher altitudes (Figure 4c, d) resulted in landscapes with biomass of 310 t/ha in the WB2.5 and almost 250 t/ha in the WB2.0 simulation at the lowest elevations, decreasing slightly with elevation over the first 600 m in the WB2.5 and 400 m in the WB2.0 simulation, but then it started to decrease quickly until about 3600 m. With increasing altitude, species composition in the two WB simulations exhibited a shift from *Pseudotsuga menziesii–Pinus contorta* to *Picea engelmannii–Abies lasiocarpa* forests. Forests near treeline were dominated by low amounts of *A. lasiocarpa* (Figure 4c, d). In Figure 5, the composition of the two high fire frequency scenarios (LHC2.0 and WB2.0) is compared to the observed situation (Sibold 2001; Sibold et al. in review; USDA Forest Service 2001). Since we were unable to derive reliable biomass estimates from the available data, only relative vegetation composition is presented.

Stand recovery after fire

At lower elevations, some trees survived the fire disturbances, mainly big *Pinus ponderosa* and some *Pseudotsuga menziesii* individuals (Figure 6a, b). At higher elevations, simulated fires killed all trees (Figure 6c, d), resulting in large amounts of dead biomass (Figure 6e, h).

After fire, simulated live aboveground biomass increased during 100–200 years (stand re-initiation
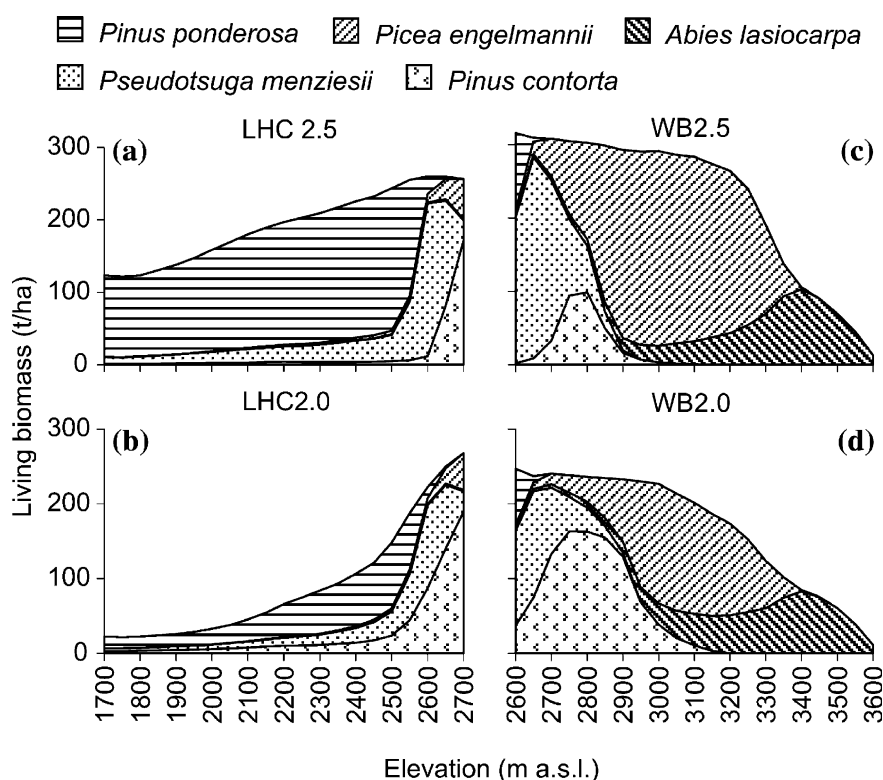
Pinus ponderosa   Picea engelmannii   Abies lasiocarpa

Pseudotsuga menziesii   Pinus contorta

Figure 4. Elevational gradient of simulated living biomass (abbreviations cf. Table 1).

and growth). Then, biomass was reduced again and leveled off at values slightly below the transitory maximum (Figure 6a, d).

Simulated dead aboveground biomass was high immediately after fire. During subsequent decades, it decreased and then increased again during the self-thinning period. After reaching a transitory maximum (e.g. at 150 years at elevations 2600–2700 m), dead biomass dropped again, followed by an increase towards a new steady-state.

Properties of the fire regime

Simulated fires were highly variable in size and frequency, with a high proportion of small fires, being typical for percolation processes (Figure 7). The majority of simulated fires was smaller than 1 ha. More fires and more larger fires were simulated at lower (LHC) than at higher elevations (WB) because of drier site conditions. Fires > 100 ha occurred on average every 50 and 8 years in the LHC2.5 and the LHC2.0 simulation, respectively. In WB, such large fires were simulated every 1040 and 80 years for WB2.5 and WB2.0, respectively (Figure 7).

Fire activity decreased with elevation in both areas. At the lowest elevations, it took ≈60 years in the LHC2.5 and 10 years in the LHC2.0 simulation to burn an area the size of the entire elevation band (Figure 8a, b). In the LHC2.5 simulation, this so-called fire rotation increased to ≈550 years at 2400–2500 m (Figure 8a), and to ≈3000–5000 years above 2500 m. In the LHC2.0 simulation, fire rotation increased to 35 years at 2400–2500 m and 150 years at the highest elevations (Figure 8b).

Fire rotation in the WB2.5 simulation was almost 4000 years at the lowest elevations and increased quickly to very high values. In contrast, the WB2.0 simulations resulted in fire rotations of 100 years at the lowest elevations and around 140–150 years above 3000 m a.s.l.
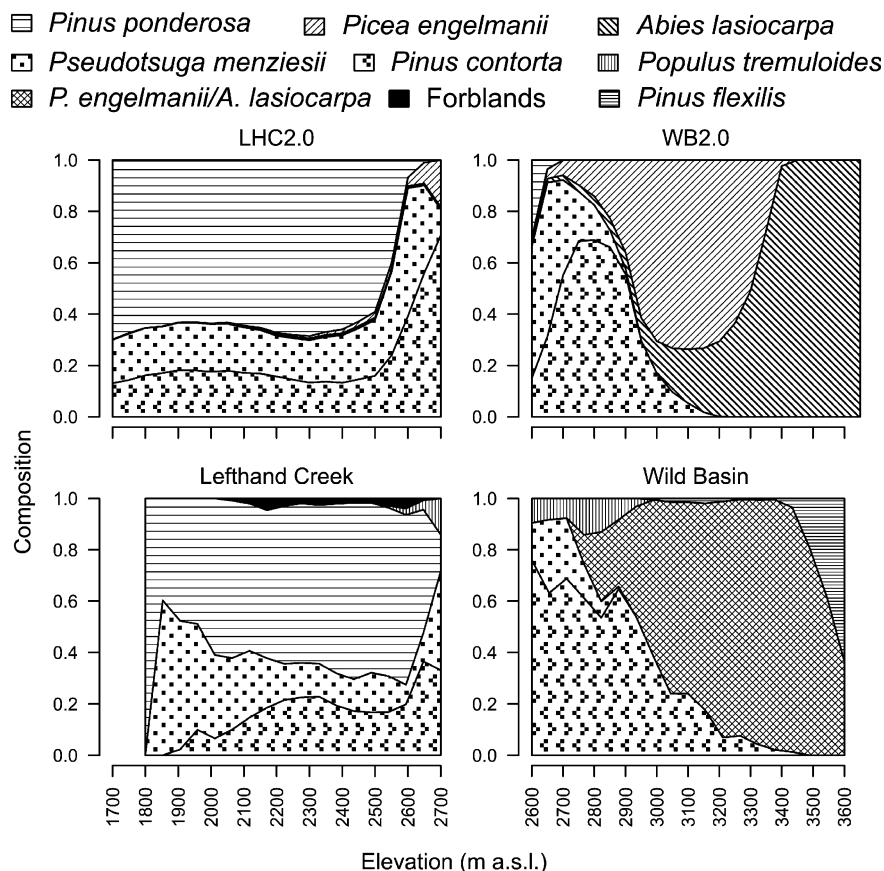
Figure 5. Elevational gradient of vegetation composition for the two simulation scenarios (top) and the empirical situation (bottom) in the two study areas (abbreviations cf. Table 1).

Discussion

Live aboveground biomass and vegetation distribution

The simulated biomass distribution is determined not only by the climatic gradient, but also by the fire activity. At low elevations, biomass values were up to sixfold larger under the LHC2.5 simulation, which experienced few fires, compared to the LHC2.0 simulation (Figures 4a, b and 8a, b). The relative difference in biomass decreased with increasing elevation. At 2250 m, live aboveground biomass averaged 210 t/ha in the LHC2.5 scenario and 90 t/ha in the LHC2.0 scenario. This range compares favorably with values observed by Hall et al. (2005) at 14 *Pinus ponderosa* sites in the Colorado Front Range, with an average 105 t/ha (range: 50–400 t/ha) at a mean elevation of 2240 m. Correspondence between simulated and

observed live aboveground biomass was also close in the subalpine zone. Measurements by Binkley et al. (2003) in 18 subalpine stands in the Colorado Front Range resulted in an average stand biomass of 250 t/ha (range: 130–490 t/ha) at a mean elevation of 3240 m; corresponding simulated mean values were 150 t/ha (WB2.0) and 270 t/ha (WB2.5).

The simulated compositional change of vegetation along the elevational gradient corresponds well to general expectations and the specific empirical situation in the two test areas (Figure 5). The lower montane zone of the Colorado Front Range is characterized by open, park-like *Pinus ponderosa* forests that become denser with increasing elevation up to *c.* 2000–2500 m (Peet 1981). *Pseudotsuga menziesii* also grows in the montane zone, occupying less xeric, cooler sites than *P. ponderosa* (Peet 2000; Steinberg 2002). With decreasing fire activity, a transition from
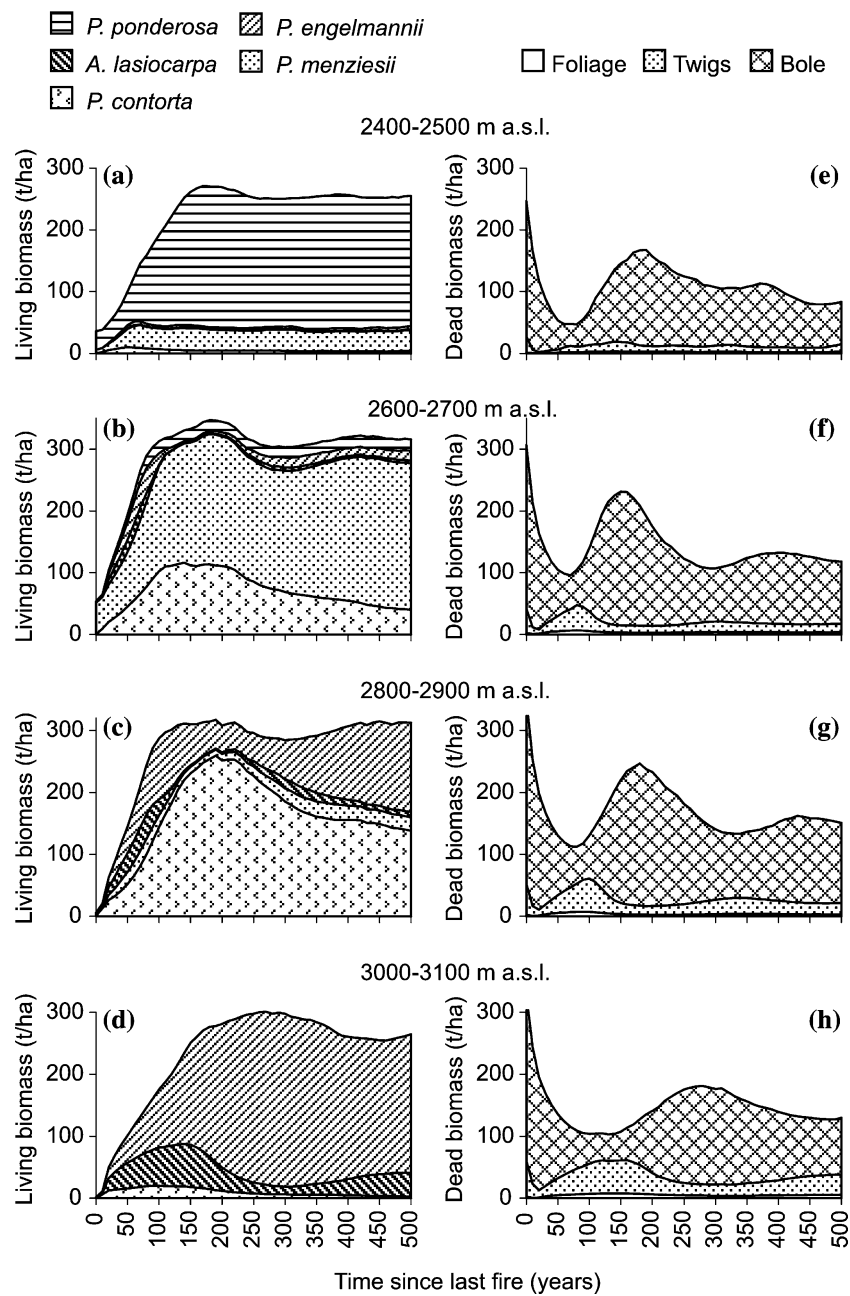
Figure 6. Stand development after fire disturbance over 500 years for selected 100 m elevation bands. *Left*: live aboveground biomass; *Right*: dead aboveground biomass.

P. ponderosa stands to forests dominated by the more shade-tolerant *P. menziesii* is expected (e.g. Korb and Ranker 2001). LANDCLIM simulated dominance by *P. menziesii* only at elevations higher than 2500 m in the less fire-affected simulations (Figure 4a, c), which may not be quite realistic (Peet 1981). We surmise that the estimation of some species-specific parameters may not have been accurate enough to correctly simulate the location of *P. menziesii* along the gradient.

P. ponderosa and *P. menziesii* co-dominate dense stands in the mixed conifer zone (ca. 2500–
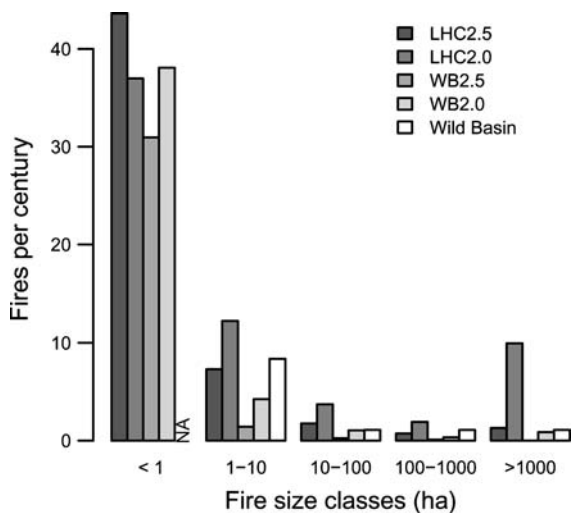
Figure 7. Simulated fire size distribution in the two study areas (abbreviations cf. Table 1), and observed data for Wild Basin.

2700 m). With increasing elevation, also *Pinus contorta* occurs in these mixed stands (Peet 1981). This pattern is matched well by the model Figure 4), as the simulated biomass value of *P. contorta* varies with simulated fire activity, and *P. contorta* was correctly simulated as an early seral species (Figure 6b, c).

The subalpine forest zone (ca. 2700–3500 m) of the Rocky Mountains in Colorado is dominated by a mixture of *P. contorta* (at lower elevations), *Picea engelmannii* and *Abies lasiocarpa* (Peet 1981); *Picea* often has the largest fraction of biomass (Aplet et al. 1989; Peet 2000; Binkley et al. 2003). For example, in the subalpine stands investigated by Binkley et al. (2003), *P. engelmannii* accounted for more than 65% of biomass, *A. lasiocarpa* for 30%, and *Pinus contorta* for <5%. The highest elevations in the Wild Basin, up to treeline, are dominated by *Pinus flexilis* (Figure 5). In the simulations, these areas were dominated by *A. lasiocarpa*, since *P. flexilis* was not included in the simulations. *Abies lasiocarpa* is often dominant at upper treeline, which is located at about 3500 m a.s.l. (Peet 2000). While species composition and biomass distribution of subalpine forests are simulated quite accurately, the elevation of simulated treeline is overestimated by about 100 m. This is most likely due to an inaccurate estimation of the species-specific minimum degree-day requirement of *A. lasiocarpa*.

Thus, the sequence of forest types along the elevational gradients was simulated well, and

differences in the location of ecotones between simulations and field data appear to be within the range of natural variability.

Development of dead biomass

The simulated dead biomass accumulation closely follows one of the theoretical debris accumulation patterns identified by Harmon et al. (1986, Figure 10B, p. 208). Initial mass is composed of dead biomass present before the disturbance and the biomass created by the disturbance. Then, a 'U'-shaped trough occurs as the stand matures, the pre- and post-disturbance debris is largely decayed, but the new stand has not produced much new coarse woody debris. The amount of dead biomass then starts to increase by stem exclusion, and finally a new equilibrium is reached.

Comparing the simulated values to the available data (Harmon et al. 1986), it is likely that the model overestimated dead biomass, which amounts to about 50% of living biomass in the simulations (Figure 6a, d). However, this ratio is not beyond the range of published data: Agee and Huff (1987) reported dead biomass values (including logs and snags) that amounted to about 35, 70, and 50% of living biomass in 110, 181, and 515 years old forest stands, respectively.

Simulated fire regime

A fire regime study in the montane zone (ca. 1830–2790 m) of the eastern slope of the northern Colorado Front Range identified 27 years with 'widespread' fires over the period 1650–1920 AD (Veblen et al. 2000), corresponding to approximately 10 widespread fires per century. Assuming these events represent fires larger than 1000 ha, the simulation LHC2.0 relates very well to these data, but the LHC2.5 simulations are underestimating the occurrence of large fires. For the subalpine Wild Basin, fire areas were reconstructed for the period 1654–1920, with three fires in each of the three largest size classes considered (10–100, 100–1000, and >1000 ha; Sibold 2001; Sibold et al. in review). Furthermore, 'single-tree fires' were identified, i.e. fires whose exact extent is not known, but that would likely have been <10 ha. In the area, 23 such fires occurred per century
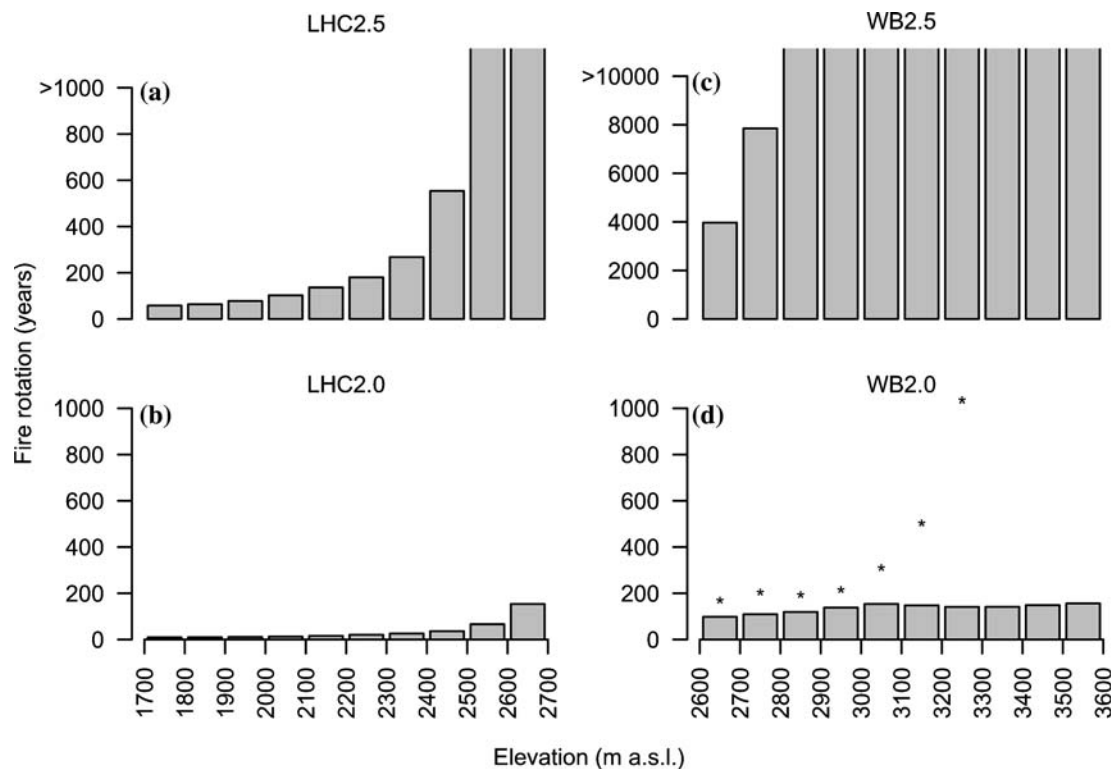
Figure 8. Elevational gradient of simulated fire rotations (abbreviations cf. Table 1). Asterisks in the bottom right panel indicate reconstructed fire rotation times from Sibold et al. (in review).

(Sibold and Veblen, unpublished data). The WB2.0 simulation resulted in a fire size distribution that is comparable with these fire records, although small fires were possibly overestimated and large fires slightly underestimated, whereas in WB2.5 the occurrence of large fires was underestimated substantially (Figure 7).

For the montane zone, only fire return intervals are available (e.g. 29 years for open *P. ponderosa* stands in the lower montane zone of the Colorado Front Range; Veblen 2000). They are not directly comparable with the simulated fire rotation data; thus we cannot validate the model results for the montane zone. The fire rotation for Wild Basin forests was estimated as 308 years (Sibold 2001). Estimated fire rotation in subalpine spruce-fir forests in northwestern Colorado is 521 years (Veblen et al. 1994), in north-central Colorado forests with a mixture of spruce-fir and lodgepole pine 346 years (Buechling and Baker 2004), and in southern Wyoming lodgepole pine forests 182 years (Kipfmueller and Baker 2000). These values are considerably smaller than the simu-

lated fire rotation under the WB2.5 simulation (Figure 8c) and somewhat higher than the WB2.0 simulation. Thus, the model captures the range of observed fire rotations, with the WB2.0 scenario being closer to reality than WB2.5.

Fire activity decreases quickly with elevation in *P. ponderosa* forests of the Colorado Front Range (Veblen et al. 2000; Stohlgren et al. 2002), but no data are available on the exact change of fire rotation with elevation in these forests. Reconstructed fire rotations for the subalpine Wild Basin show an exponential increase with elevation (Sibold et al. in review; Figure 8). While LAND-CLIM exhibits such an exponential increase for the montane area (LHC), the simulated increase is much weaker and nearly linear for WB2.0 (Figure 8).

Overall, LANDCLIM captured key characteristics of the observed fire regime in the two study areas, but due to the large uncertainty and high sensitivity of the model to the fire probability parameter, we cannot unequivocally verify (or falsify) model behavior.

The simulation results show that the shape of the fire probability curve [Eq. (1)] is a crucial determinant of fire behavior. In LANDCLIM, a percolation process based on probabilities that are dependent on soil water content determines fire occurrence and size. It is well known that spread behavior is restricted to a fairly narrow range of probabilities (Stauffer and Aharony 1995). Below a certain threshold, fire is unable to spread (probability < 0.25 in the case of 8 neighboring cells; Figure 2). Above a percolation threshold of ≈ 0.4 (for percolation to 8 cells), fire always spreads across the entire landscape (Stauffer and Aharony 1995; Hargrove et al. 2000). Hence, small changes in the fire spread probability curve (Figure 2) can have drastic impacts on the fire regime and thus on forest composition. The model's high sensitivity to the percolation probabilities makes it necessary to either estimate the fire-spread probability function very carefully based on an extensive set of data (which is not available to us at the moment); or to account for the range of uncertainty when setting up simulations and interpreting simulation results. Although we were able to narrow down the range of plausible shapes of the fire probability curve using a sensitivity study (Schumacher 2004), its exact shape should be the subject of further research. Such a model improvement would be particularly valuable for accurately simulating the *Pinus contorta–Picea engelmannii/Abies lasiocarpa* zone in the Rocky Mountains, where fire frequency maintains a delicate balance between early-seral *P. contorta* and late-seral *P. engelmannii* and *A. lasiocarpa* (Romme and Knight 1981).

Conclusions

In this study, LANDCLIM was tested for its ability to simulate the interaction between climatic conditions, fire disturbances and forest composition along an extended altitudinal gradient (1700 m to upper treeline) in the Colorado Front Range.

The structure of LANDCLIM was found to be suitable for simulating the responses of fire and vegetation properties to environmental conditions. Particularly, no predetermined fire frequency and size distribution are required to run the fire submodel; they result as emergent properties of climate and ecological interactions. Variations in climatic parameters and the topographic setting result in a different fire regime. At the same time, forest composition is affected directly by climatic and soil conditions, and indirectly by fire. This general structure makes the model applicable to a broad range of landscapes. However, further research is required to reduce to the large uncertainty of the fire probability parameter (*fireExp*), as model behavior is highly sensitive to its value.

Overall, the model presented here can be useful for exploring the relative differences of the fire regime between climatic regimes, and to assess the responses of forest landscapes to variations in climatic parameters from the dry to the cold treeline. Thus, the model could be applied for improving our understanding of the impacts of a changing climate on potential fire regime shifts while simultaneously considering the long-term effects on and the interaction with vegetation dynamics.

References

Agee J.K. and Huff M.H. 1987. Fuel succession in a western hemlock/Douglas-fir forest. Can. J. For. Res. 17: 697–704.

Albini F.A. 1976. Estimating wildfire behavior and effects. USDA Forest Service General Technical Report INT-30.

Anderson M.D. 2003. *Pinus contorta* var. *latifolia*. In: Fire Effects Information System, [Online]. U.S. Department of Agriculture, Forest Service, Rocky Mountain Research Station, Fire Sciences Laboratory (Producer). Available: http://www.fs.fed.us/database/feis.

Aplet G.H., Smith F.W. and Laven R.D. 1989. Stemwood biomass and production during spruce-fir stand development. J. Ecol. 77: 70–77.

Arno S.F. 2000. Fire in western forest ecosystems. In: Brown J.K. and Smith J.K. (eds), Wildland Fire in Ecosystems: Effects of fire on flora Gen. Tech. Rep. RMRS-GTR-42-Vol. 2 Ogden. U.S. Department of Agriculture, Forest Service, Rocky Mountain Research Station, UT, pp. 97–120.

Baker W.L., Egbert S.L. and Frazier G.F. 1991. A spatial model for studying the effects of climatic change on the structure of landscapes subject to large disturbances. Ecol. Model. 5: 109–125.

Bessie W.C. and Johnson E.A. 1995. The relative importance of fuels and weather on fire behavior in subalpine forests. Ecology 76: 747–762.

Binkley D., Olsson U., Rochelle R., Stohlgren T. and Nikolov N. 2003. Structure, production and resource use in some old-growth spruce/fir forests in the Front Range of the Rocky Mountains, USA. For. Ecol. Manage. 172: 271–279.

Botkin D.B. 1993. Forest Dynamics: An Ecological Model. Oxford University Press, Oxford & New York.

Brown J.K. 2000. Ecological principles, shifting fire regimes and management considerations. In: Brown J.K. and Smith J.K. (eds), Wildland Fire in Ecosystems: Effects of Fire on Flora. Gen. Tech. Rep. RMRS-GTR-42-Vol. 2 Ogden. U.S. Department of Agriculture, Forest Service, Rocky Mountain Research Station, UT, pp. 185–203.

Brown J.K., Reinhardt E.D. and Fischer W.C. 1991. Predicting duff and woody fuel consumption in northern Idaho prescribed fires. For. Sci. 37: 1550–1566.

Buechling A. and Baker W.L. 2004. A fire history from tree rings in a high-elevation forest of Rocky Mountain National Park. Can. J. For. Res. 34: 1259–1273.

Bugmann H. 1994. On the ecology of mountainous forests in a changing climate: a simulation study. PhD Thesis, No. 10638, Swiss Federal Institute of Technology Zurich, Switzerland, 258 pp.

Bugmann H. 2001. A comparative analysis of forest dynamics in the Swiss Alps and the Colorado Front Range. For. Ecol. Manage. 145: 43–55.

Bugmann H. and Cramer W. 1998. Improving the behaviour of forest gap models along drought gradients. For. Ecol. Manage. 103: 247–263.

Bugmann H.K.M. and Solomon A.M. 2000. Explaining forest composition and biomass across multiple biogeographical regions. Ecol. Appl. 10: 95–114.

Burns R.M. and Honkala B.H. (eds) 1990. Silvics of North America: 1 Conifers. Agriculture Handbook 654. Vol. 2. U.S. Department of Agriculture Forest Service, Washington, DC.

Christensen O. 1977. Estimation of standing crop and turnover of dead wood in a Danish oak forest. Oikos 28: 177–186.

Ellenberg H. 1996. Vegetation Mitteleuropas mit den Alpen in ökologischer, dynamischer und historischer Sicht. Ulmer, Stuttgart.

Fahnestock G.R. and Agee J.K. 1983. Biomass consumption and smoke production by prehistoric and modern forest fires in western Washington. J. For. 81: 653–656.

Finney M.A. 1998. FARSITE: Fire Area Simulator-model Development and Evaluation. USDA Forest Service Research Paper RMRS-RP-4, 47 pp.

Gardner R.H., Romme W.H. and Turner M.G. 1999. Predicting forest fire effects at landscape scales. In: Mladenoff D.J. and Baker W.L. (eds), Spatial Modeling of Forest Landscpae Change: Approaches and Applications. Cambridge University Press, Cambridge, AO, pp. 163–185.

Hall S.A., Burke I.C., Box D.O., Kaufmann M.R. and Stoker J.M. 2005. Estimating stand structure using discrete-return lidar: an example from low density, fire prone ponderosa pine forests. For. Ecol. Manage. 208: 189–209.

Hargrove W.W., Gardner R.H., Turner M.G., Romme W.H. and Despain D.G. 2000. Simulating fire patterns in heterogeneous landscapes. Ecol. Model. 135: 243–263.

Harmon M.E., Franklin J.F. and Swanson F.J. et al. 1986. Ecology of coarse woody debris in temperate ecosystems. Adv. Ecol. Res. 15: 133–300.

He H.S. and Mladenoff D.J. 1999a. The effects of seed dispersal on the simulation of long-term forest landscape change. Ecosystems 2: 308–319.

He H.S. and Mladenoff D.J. 1999b. Spatially explicit and stochastic simulation of forest-landscape fire disturbance and succession. Ecology 80: 81–99.

Hefti R., Schmid-Haas P. and Bühler U. 1986. Zustand und Gefährdung der Davoser Waldungen. MAB-Schlussberichte23. Bundesamt für Umweltschutz, Bern.

Heinimann H.R., Hollenstein K., Kienholz H. and Krummenacher B. 1998. Methoden zur Analyse und Bewertung von Naturgefahren Umwelt-Materialien Nr. 85 Naturgefahren. Bundesamt für Umwelt, Wald und Landschaft (BUWAL), Bern.

Hillgarter F.-W. 1971. Waldbauliche und ertragskundliche Untersuchungen im subalpinen Fichtenurwald Scatlé/Brigels. PhD Thesis, No. 4619, Swiss Federal Institute of Technology Zurich, Switzerland.

Howard J.L. 2003. *Pinus ponderosa* var. *scopulorum*. In: Fire Effects Information System, [Online]. U.S. Department of Agriculture, Forest Service, Rocky Mountain Research Station, Fire Sciences Laboratory (Producer), Available: http://www.fs.fed.us/database/feis.

IPCC 2001. Climate change 2001: The scientific basis. In: Houghton J.T.Ding Y. and Griggs D.J. et al. (eds), Contribution of Working Group I to the Third Assessment Report of the Intergovernmental Panel on Climate Change. Cambridge University Press, Cambridge and New York.

Johnson E.A. 1992. Fire and Vegetation Dynamics: Studies from the North American Boreal Forest. Cambridge University Press, Cambridge.

Keane R.E., Cary G.J. and Davis I.D. et al. 2004. A classification of landscape fire succession models: spatial simulations of fire and vegetation dynamics. Ecol. Model. 179: 3–27.

Keane R.E., Morgan P. and Running S.W. 1996. FIRE-BGC – A Mechanistic Ecological Process Model for Simulating fire Succession on Coniferous Forest Landscapes of the Northern Rocky Mountains. USDA Forest Service Research Paper INT-RP-484, Ogden, Utah.

Kipfmueller K.F. and Baker W.L. 2000. A fire history of a subalpine forest in south-eastern Wyoming, USA. J. Biogeogr. 27: 71–85.

Korb J.E. and Ranker T.A. 2001. Changes in stand composition and structure between 1981 and 1996 in four Front Range plant communities in Colorado. Plant Ecol. 157: 1–11.

Körner C. 1998. A re-assessment of high elevation treeline positions and their explanation. Oecologia 115: 445–459.

Mackensen J., Bauhus J. and Webber E. 2003. Decomposition rates of coarse woody debris – A review wit particular emphasis on Australian tree species. Aust. J. Bot. 51: 27–37.

Meentemeyer V. 1978. Macroclimate and lignin control of litter decomposition rates. Ecology 59: 465–472.

Nash C.H. and Johnson E.A. 1996. Synoptic climatology of lightning-caused forest fires in subalpine and boreal forests. Can. J. For. Res. 26: 1859–1874.

Oliver C.D. and Larson B.C. 1996. Forest Stand Dynamics. John Wiley & Sons Inc., New York, AO.

Paulsen J. 1995. Der biologische Kohlenstoffvorrat der Schweiz. Rüegger, Chur, AO.

Peet R.K. 1981. Forest vegetation of the Colorado Front Range: composition and dynamics. Vegetatio 37: 65–78.

Peet R.K. 2000. Forests and meadows of the Rocky Mountains. In: Barbour M.G. and Billings W.D. (eds), North American Terrestrial Vegetation. Cambridge University Press, Cambridge, AO, pp. 75–121.

Romme W.H. and Knight R.L. 1981. Fire frequency and subalpine forest succession along a topographic gradient in Wyoming. Ecology 62: 319–326.

Rothermel R.C. 1972. A Mathematical Model for Predicting Fire Spread in Wild Land Fuels. USDA Forest Service, Intermountain Forest and Range Experiment Station Research Paper, INT-115, Ogden, UT.

Ryan K.C. and Reinhardt E.D. 1988. Predicting postfire mortality of seven western conifers. Can. J. For. Res. 18: 1291–1297.

Schroeder P., Brown S., Mo J., Birdsey R. and Cieszewski C. 1997. Biomass estimation for temperate broadleaf forests of the United States using inventory data. For. Sci. 43: 424–434.

Schumacher S. 2004. The role of large-scale disturbances and climate for the dynamics of forested landscapes in the European Alps. PhD Thesis, No. 15573, Swiss Federal Institute of Technology Zurich, Switzerland. Available: http://e-collection.ethbib.ethz.ch/show?type = diss&nr = 155 73, 141 pp.

Schumacher S., Bugmann H. and Mladenoff D.J. 2004. Improving the formulation of tree growth and succession in a spatially explicit landscape model. Ecol. Model. 180: 175–194.

Sibold J.S. 2001. The forest fire regime of an upper montane and subalpine forest, Wild Basin, Rocky Mountain National Park. MA Thesis, University of Colorado, Boulder, CO.

Sibold J.S., Veblen T.T. and Gonzalez M.E. 2005. Spatial and Temporal Variation in Historic Fire Regimes in Subalpine Forests across the Colorado Front Range in Rocky Mountain National Park. J. Biogeogr. (in press).

SMA 2003. Annalen der Schweizerischen Meteorologischen Anstalt. Swiss Meteorological Agency, Zürich.

Stauffer D. and Aharony A. 1995. Perkolationstheorie – Eine Einführung. VHC Verlagsgesellschaft, Winheim, AO.

Steinberg P.D. 2002. *Pseudotsuga menziesii* var. *glauca*. In: Fire Effects Information System, [Online]. U.S. Department of Agriculture Service, Forest Service, Rocky Mountain Research Station, Fire Sciences Laboratory (Producer), Available: http://www.fs.fed.us/database/feis.

Stohlgren T.J., Veblen T.T., Kendall K.C., Baker W.L., Allen C.D., Logan J.A. and Ryan K.C. 2002. The heart of the Rockies: mountain and subalpine ecosystems. In: Baron J.S. (ed.), Rocky Mountain Futures: An Ecological Perspective. Island Press, Washington, AO, pp. 203–218.

Swetnam T.W. and Betancourt J.L. 1990. Fire-southern oscillation relations in the southwestern USA. Science 249: 1017–1020.

Uchytil R.J. 1991a. *Abies lasiocarpa*. In: Fire Effects Information System [Online]. U.S. Department of Agriculture, Forest Service, Rocky Mountain Research Station, Fire Sciences Laboratory (Producer), Available: http://www.fs.fed.us/database/feis.

Uchytil R.J. 1991b. *Picea engelmannii*. In: Fire Effects Information System [Online]. U.S. Department of Agriculture, Forest Service, Rocky Mountain Research Station, Fire Sciences Laboratory (Producer), Available: http://www.fs.fed.us/database/feis.

USDA Forest Service 2001. Arapaho and Roosevelt National Forest Geographic Information System.

Van Wagner C.E. 1973. Height of crown scorch in forest fires. Can. J. For. Res. 3: 373–378.

Veblen T.T. 2000. Disturbance patterns in southern Rocky Mountain forests. In: Knight R.L., Smith F.W., Buskirk S.W., Romme W.H. and Baker W.L. (eds), Forest Fragmentation in the Southern Rocky Mountains. University Press of Colorado, Boulder, pp. 31–54.

Veblen T.T., Hadley K.S., Nel E.M., Kitzberger T., Reid M. and Villalba R. 1994. Disturbance regime and disturbance interactions in a Rocky Mountain subalpine forest. J. Ecol. 82: 125–135.

Veblen T.T., Kitzberger T. and Donnegan J. 2000. Climatic and human influences on fire regimes in Ponderosa pine forests in the Colorado Front Range. Ecol. Appl. 10: 1178–1195.

Yoda K., Kira T., Ogawa H. and Hozumi K. 1963. Self-thinning in overcrowded pure stands under cultivated and natural conditions. J. Biol. Osaka City University, 107–129.

Zumbühl G. and Burnand J. 1986. Vegetationskarte Davos – Parsenn – Dischma. In: Wildi O. and Ewald K. (eds), Der Naturraum und dessen Nutzung im alpinen Tourismusgebiet von Davos. Ergebnisse des MAB-Projektes Davos. Berichte. Eidg. Anstalt für das forstliche Versuchswesen, Birmensdorf, pp. 139–173.